Phys. Status Solidi A **213,** No. 11, 2844–2849 (2016) / **DOI** 10.1002/pssa.201600360

physica status solidi a
www.pss-a.com
applications and materials science

Permanent annihilation of thermally activated defects which limit the lifetime of float-zone silicon

Nicholas E. Grant*[,1], Vladimir P. Markevich[2], Jack Mullins[2], Anthony R. Peaker[2], Fiacre Rougieux[3], Daniel Macdonald[3], and John D. Murphy[1]

[1] School of Engineering, University of Warwick, Coventry CV4 7AL, United Kingdom
[2] Photon Science Institute and School of Electrical and Electronic Engineering, University of Manchester, Manchester M13 9PL, United Kingdom
[3] Research School of Engineering, College of Engineering and Computer Science, Australian National University, Canberra ACT 2601, Australia

Received 29 April 2016, revised 20 May 2016, accepted 10 June 2016
Published online 1 July 2016

Keywords defects, float-zone crystal growth, heat treatment, minority carrier lifetime, silicon, vacancies

* Corresponding author: e-mail nicholas.e.grant@warwick.ac.uk, Phone: +44 247 652 8590

We have observed very large changes in the minority carrier lifetime when high purity float-zone (FZ) silicon wafers are subject to heat-treatments in the range of 200–1100 °C. Recombination centres were found to become activated upon annealing at 450–700 °C, causing significant reductions in the bulk lifetime, detrimental for high efficiency solar cells and stable high powered devices. Photoluminescence imaging of wafers annealed at 500 °C revealed concentric circular patterns, with lower lifetimes occurring in the centre, and higher lifetimes around the periphery. Deep level transient spectroscopy measurements on samples extracted from the centre of an *n*-type FZ silicon wafer annealed at 500 °C revealed a large variety of defects with activation energies ranging between 0.16–0.36 eV. Our measurements indicate that vacancy related defects are causing the severe degradation in lifetime when FZ wafers are annealed at 450–700 °C. Upon annealing FZ silicon at temperatures >800 °C, the lifetime is completely recovered, whereby the defect-rich regions vanish and do not reappear (permanently annihilated). Our results indicate that, in general, as-grown FZ silicon should not be assumed to be defect lean, nor can it be assumed that the bulk lifetime will remain stable during thermal processing, unless annealed at temperatures >1000 °C.

1 Introduction Float-zone (FZ) silicon is a commonly used material for the fabrication of very high efficiency (>24%) laboratory solar cells, and power devices where the requirement for pure (oxygen lean) silicon is essential. Because there is no crucible used in the FZ process, very high purities can be achieved and in particular low oxygen concentrations. In Czochralski (Cz) grown silicon, oxygen tends to precipitate during high temperature processing of solar cells and power devices (including dopant diffusion processes), and the precipitates negatively impact the lifetime/performance of the finished device [1–4]. In contrast, silicon from the FZ process is effectively immune to such oxygen-related lifetime-degradation during high temperature processing, thus making FZ an ideal material for high performance devices.

The common assumption that FZ silicon is defect lean has largely restricted the examination of recombination active grown-in defects to Cz and multicrystalline silicon. Recently, however, we have found significant changes in the lifetime of commercially available FZ silicon wafers when subject to heat-treatments over the range 200–1100 °C [5–8]. These changes have been attributed to the transformation of grown-in defects, primarily vacancies, which are linked to strong recombination activity after annealing at temperatures of 450–700 °C. Although such defects in nitrogen-doped (commercial standard) FZ silicon cannot be detected through X-ray topography [9], our sensitive photoconductance-based lifetime characterisation methods demonstrate that as-grown FZ silicon still contain a large number of recombination active defects, which can have a detrimental

effect on the performance of high efficiency solar cells and stable high powered devices.

In this work, we use a sensitive minority carrier lifetime measurement technique to examine the activation and permanent deactivation of recombination-active defects by heat-treatments over a wide temperature range of 200–1100 °C. We perform photoluminescence imaging to detect spatial non-uniformities in the bulk lifetime when the defects are activated. Finally, the defects are examined by deep level transient spectroscopy (DLTS).

2 Experimental The samples under investigation were (100) orientation float-zone (FZ) silicon wafers and their diameter was 100 mm. Details of the samples investigated are outlined in Table 1.

The wafers were cleaved into quarters, etched in a 1% HF solution and then RCA cleaned. Following the RCA clean and a subsequent 1% HF dip (to remove the chemically grown oxide), the samples were loaded into a clean quartz tube furnace and annealed at the set temperature for 30 min in dry oxygen with a flow rate of $\sim$15 l hr^{-1}. For temperatures higher than 700 °C, there was an additional ramp up and cool down period. The ramp up and cool down rates were $\sim$20 °C min^{-1}.

To examine the impact of annealing temperature on the bulk lifetime, minority carrier lifetime measurements were performed using a room temperature surface passivation technique [10, 11]. In this technique, silicon wafers are immersed in a container filled with 170 ml of 15 wt.% hydrofluoric acid-hydrochloric acid (HF-HCl) solution (100 ml of H_2O, 50 ml of 48% HF and 20 ml of 37% HCl) and centred over an inductive coil for transient photoconductance (PC) measurements (using a WCT-120 system from Sinton Instruments) [12]. To activate the surface passivation, the wafers are illuminated at 0.2 suns for 1 min using a halogen lamp. The light source is then switched off, and a transient lifetime measurement is immediately performed. To achieve a very low surface recombination velocity (S) of less than 1 cm s^{-1} on n- and p-type silicon, the wafers were chemically treated prior to immersing the wafers into the HF-HCl solution. The chemical treatment involved two steps: (1) the wafers were cleaned by the standard RCA procedure and (2) subsequently etched in 25 wt.% tetramethylammonium hydroxide (TMAH) at 80–90 °C for 5 min (removing about 2.5 μm of silicon per side). This chemical treatment ensures the silicon surface is defect and contaminant lean prior to surface passivation.

Table 1 FZ materials used in this work.

manufacturer	resistivity ($\Omega \cdot$ cm)	doping type	thickness (μm)	nitrogen (cm^{-3})
A	1.5	n	200	5.0×10^{14}
B	>100	n	400	4.0×10^{14}
B2	1	n	200	10^{14}–10^{15}[a]
C	5	n	150	10^{14}–10^{15}[a]
D	2	p	300	1.0×10^{15}
D	1.5	n	500	N lean[b]
E	>100	p	300	N lean

The nitrogen concentration was determined by SIMS and the resistivity is as quoted by the manufacturers.
[a]Estimated by the manufacturer but not measured.
[b]Confirmed by the manufacturer.

To investigate the spatial non-uniformity of the bulk lifetime using photoluminescence imaging, some wafers were passivated with a 20 nm atomic layer deposited (ALD) aluminium oxide (Al_2O_3) film. Prior to the depositions, all samples received a standard RCA clean. The Al_2O_3 films were deposited at 175 °C using a Beneq TFS200 ALD system at ANU. Post deposition, the Al_2O_3 films were annealed in forming gas at 400 °C for 30 min to activate the surface passivation.

For DLTS measurements, 1 mm diameter Schottky diodes were formed on n-type samples by thermal evaporation of Au, and on p-type samples by plasma sputtering of Ti through a shadow mask. A thick layer of Al(Au) was evaporated onto the back side of the samples to form an ohmic contact. Current–voltage and capacitance–voltage measurements at different temperatures were carried out in order to evaluate the quality of the diodes and to determine the concentration of uncompensated shallow acceptors/donors in the regions probed by DLTS. Deep electronic levels were characterised with conventional DLTS and high-resolution Laplace DLTS (L-DLTS) techniques [13].

The nitrogen concentration in the FZ wafers was determined by secondary ion mass spectroscopy (SIMS) measurements made by EAG. For samples with an undetectable quantity of nitrogen, we report the detection limit of the system (5×10^{13} cm^{-3}) as the upper limit.

3 Surface recombination velocity of HF-HCl passivation To measure the bulk lifetime of high quality, high lifetime silicon wafers, surface recombination must be suppressed. The following will demonstrate that HF-HCl passivation does satisfy this condition.

In order to measure the surface recombination velocity of silicon wafers immersed in a 15 wt.% HF-HCl solution, the wafer thickness variation method was employed [14]. For this method, 100 mm diameter 1 $\Omega \cdot$ cm n- and p-type FZ silicon wafers were cleaved into quarters and then thinned by etching in a 25 wt.% TMAH solution, whereby each quarter was etched to a different thickness W and then passivated by HF-HCl using the technique described in Section 2. For sufficiently low S, as is the case for HF-HCl passivation, the effective lifetime τ_{eff} can be expressed as [15]

$$\frac{1}{\tau_{\text{eff}}} = \frac{1}{\tau_{\text{bulk}}} + \frac{2S}{W},$$

whereby a plot of $1/\tau_{\text{eff}}$ against $1/W$ yields a straight line where $2S$ is the slope and $1/\tau_{\text{bulk}}$ the intercept. Figure 1 plots the results.

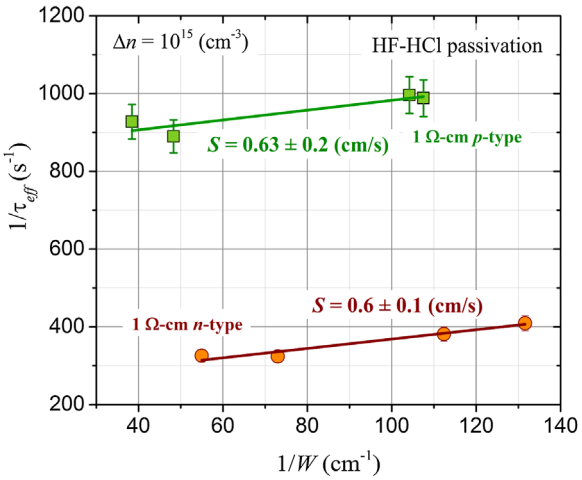

Figure 1 Inverse effective lifetime (at $\Delta n = 10^{15}\,\mathrm{cm}^{-3}$) versus inverse sample thickness for 1 Ω · cm FZ n- and p-type silicon. The error bars represent a ±5% uncertainty in the measured lifetime using transient PCD as demonstrated in Ref. [16].

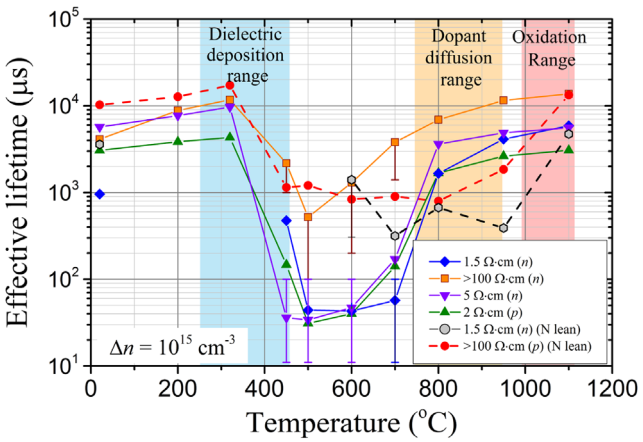

Figure 2 Effective lifetime (at $\Delta n = 10^{15}\,\mathrm{cm}^{-3}$) versus annealing temperature for six different FZ silicon ingots (five different manufacturers). Annealing was performed in dry oxygen for 30 min. Each data point corresponds to a new sample. (From Ref. [8].)

Figure 1 plots $1/\tau_{\mathrm{eff}}$ against $1/W$ for 1 Ω · cm FZ n- and p-type silicon samples immersed in a 15 wt.% HF-HCl solution. From the slope of the data, S of 0.6 cm s^{-1} is determined for both 1 Ω · cm n- and p-type silicon, thus demonstrating the HF passivation technique is very effective at suppressing surface recombination. In contrast, however, a surface recombination velocity of 0.6 cm s^{-1} can still limit the lifetime by several milliseconds when $\tau_{\mathrm{bulk}} \geq 10$ ms, and therefore we report the effective lifetime. Furthermore we choose not to correct the effective lifetime measurements using an S of 0.6 cm s^{-1}, because it is likely that S decreases with increasing resistivity as indicated by our previous results in Ref. [6] and for Al_2O_3 passivation [17].

4 Lifetime instability upon heat-treating FZ silicon (200–1100 °C) Figure 2 shows the effective lifetime versus annealing temperature of FZ silicon wafers taken from five different ingots. For each annealing temperature, new samples were used. For the lifetime shown in Fig. 2, an injection level of $\Delta n = 10^{15}\,\mathrm{cm}^{-3}$ was chosen instead of $0.1 \times N_{\mathrm{doping}}$ because such low injection levels could not be measured for some samples (i.e. >100 Ω · cm).

Prior to any thermal treatment, all samples in Fig. 2 show lifetimes in the millisecond range (1–10 ms), however, these values are well below the intrinsic limit [17], even when corrected for $S = 0.6$ cm s^{-1}, indicating the existence of grown-in defects which are causing additional bulk recombination. To highlight the existence of grown-in defects further, Fig. 3 plots the effective lifetime of 25 FZ >100 Ω · cm n-type silicon wafers (one box of wafers), which had not undergone any thermal processing post crystal growth. The wafer number in Fig. 3 represents the position of the wafer in the box, as received from the manufacturer. In this case, the nitrogen concentration in each of the wafers is unknown, however, the concentration is expected to be of the order 10^{14}–10^{15} cm^{-3} as indicated by Table 1.

Figure 3 demonstrates that in one box of 25 wafers, the lifetime can vary from wafer to wafer. Surprisingly, in most cases, the lifetime is low (5–6 ms) relative to the wafers with much higher lifetimes (shown in red) within the same box. These findings demonstrate that (i) a box of wafers does not come from the same location within the ingot and (ii) the low lifetimes suggest a recombination active grown-in defect is present in FZ silicon.

When the silicon samples shown in Fig. 2 were annealed at 200 °C and then 300 °C, a significant increase in τ_{eff} is observed for both n- and p-type silicon wafers. For example, in the case of the 5 Ω cm n-type sample, τ_{eff} increased from

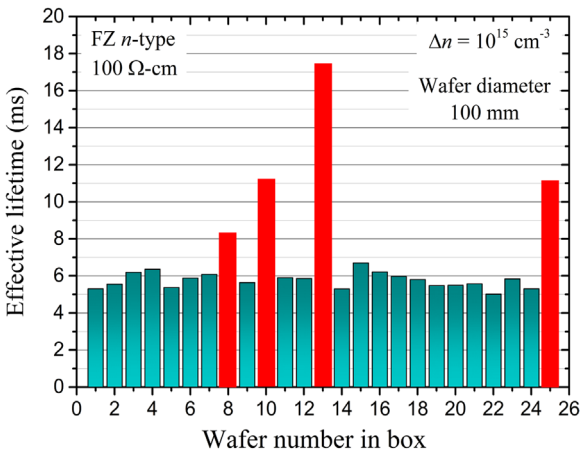

Figure 3 Effective lifetime of FZ silicon wafers as measured using the HF passivation technique [10, 11]. The wafer number represents the position of the wafer in the box, as received from the manufacturer. The nitrogen concentration was not measured in each of these samples, however, the concentration is expected to be of the order 10^{14}–10^{15} cm^{-3} as indicated in Table 1.

~5 ms in the as-grown state to ~10 ms after annealing at 300 °C. This increase in lifetime is consistent with our previous work on deactivation of defects at low annealing temperatures [5], and thus the increase in lifetime as seen in Fig. 2 is not related to surface passivation instabilities. At this time, it is unclear if the defect being deactivated at low temperatures (300–350 °C) is related to the same defect giving rise to the degradation in bulk lifetime upon annealing at 450–700 °C, however, it is interesting to note that the lifetime post annealing at 300–350 °C is generally the highest (Fig. 2).

When the FZ silicon samples were annealed in the temperature range 450–700 °C, the lifetime was found to decrease significantly, and in the worst case (5 Ω · cm n-type), τ_{eff} decreased by more than two orders of magnitude. To elucidate why a very large decrease in τ_{eff} is observed, photoluminescence (PL) images of samples annealed at 500 °C were recorded.

Figure 4 depicts a calibrated lifetime image of a nitrogen doped FZ 5 Ω · cm n-type silicon wafer annealed at 500 °C. Figure 4 clearly demonstrates that the lifetime significantly decreases and becomes spatially non-uniform, as evident from the disc/ring patterns. In Cz silicon, such ring patterns are commonly attributed to oxygen-related extended defects, however, for FZ, the rings can only be attributed to the growth conditions of the ingot and thus the lifetime patterns shown in Fig. 4 likely correspond to the distribution of vacancies [9, 18, 19]. At this time, it is unclear if nitrogen is involved in the defect reaction, however, it is known from the literature that nitrogen doping increases the vacancy concentration by preventing void formation [9], thus giving rise to a vacancy distribution that is high in the centre of the ingot and lower around the periphery, which could explain the lower lifetime in the central region of the wafer in Fig. 4. In contrast, we also point out that the lifetime around the periphery in Fig. 4 is also reduced, consistent with Refs. [6, 8], however, at this time the source of recombination is unknown.

When nitrogen-doped silicon samples were subject to heat-treatments at temperatures ≥800 °C in an oxygen ambient for 30 min, the lifetime not only recovered, but substantially improved relative to the as-grown lifetime for some wafers. At this stage, the reason for the rapid recovery in lifetime at these temperatures is unclear, however, it is clear that the vacancy defect giving rise to the disk like defect distribution shown in Fig. 4 disappear post annealing at ≥1000 °C, as shown in Fig. 5.

Figure 5 shows uncalibrated PL images of nitrogen doped silicon samples annealed at 500 °C (left) and 1000 °C (right) in oxygen for 30 min and subsequently passivated with 20 nm of ALD Al_2O_3. Each image was taken under the same illumination conditions, therefore, the yellow (bright) regions in both images do equate to the same lifetime.

Figure 5 demonstrates that when FZ silicon wafers are annealed at very high temperatures, the concentric circular defect distribution shown in the left figure disappear upon annealing at 1000 °C as shown in Fig. 5 (right). To demonstrate the permanent annihilation of the defect shown in Fig. 5 (left), silicon samples were annealed at 1000 °C and then subject to an additional anneal at 450 °C where the defect is known to arise. Figure 6 plots the results.

Figure 6 plots the effective lifetime (at $\Delta n = 10^{15}$ cm^{-3}) of nitrogen doped 1, 10 and 100 Ω · cm n-type FZ silicon (i) as-grown; (ii) after a 450 °C anneal; (iii) followed by a 1000 °C anneal and (iv) annealed once again at 450 °C. The lifetime dependence with resistivity in Fig. 6 is at least in part attributed to intrinsic recombination, which is strongly dependent on doping level [17].

Figure 6 demonstrates that when as-grown FZ silicon wafers are subject to a low temperature anneal at 450 °C, a significant decrease in the bulk lifetime arises, which we attribute to the activation of a vacancy defect as shown in Fig. 4. However, as demonstrated in Figs. 2 and 5, when the wafers are subject to a very high temperature anneal in oxygen, the lifetime not only recovers, but improves relative to the as-grown state.

To demonstrate the permanent annihilation of the vacancy defect, the wafers which had undergone a 1000 °C anneal were subject to a second anneal in oxygen at 450 °C, where previously the defect became activated. As seen in Fig. 6, no reduction in the lifetime is observed following the second 450 °C anneal, thus suggesting the

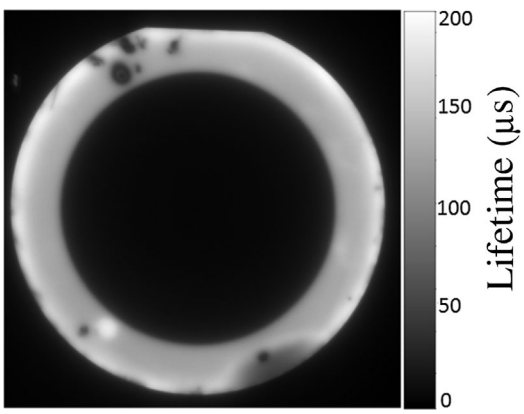

Figure 4 Calibrated lifetime image of a nitrogen doped 100 mm diameter FZ 5 Ω · cm n-type silicon wafer annealed at 500 °C. The sample was passivated by 20 nm of ALD Al_2O_3.

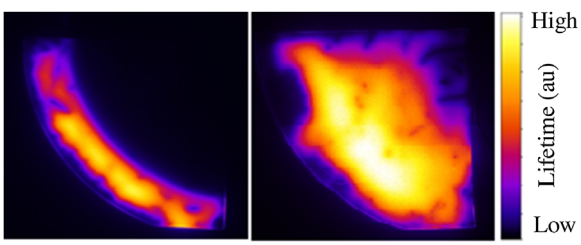

Figure 5 Uncalibrated PL images of quarter 100 mm diameter nitrogen doped FZ 100 Ω · cm n-type silicon samples annealed at 500 °C (left) and 1000 °C (right) in oxygen for 30 min. The samples were passivated by 20 nm of ALD Al_2O_3.

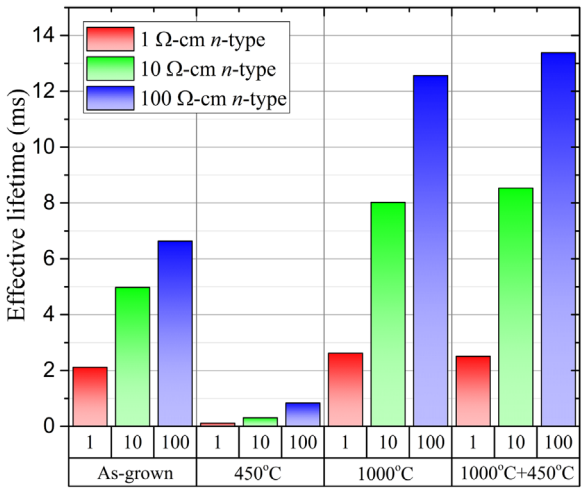

Figure 6 Effective lifetime (at $\Delta n = 10^{15}\,\mathrm{cm}^{-3}$) of nitrogen doped FZ 1 (red), 10 (green) and 100 (blue) $\Omega \cdot$cm n-type silicon (i) as-grown; (ii) after a 450 °C anneal; (iii) followed by a 1000 °C anneal and (iv) a subsequent anneal at 450 °C.

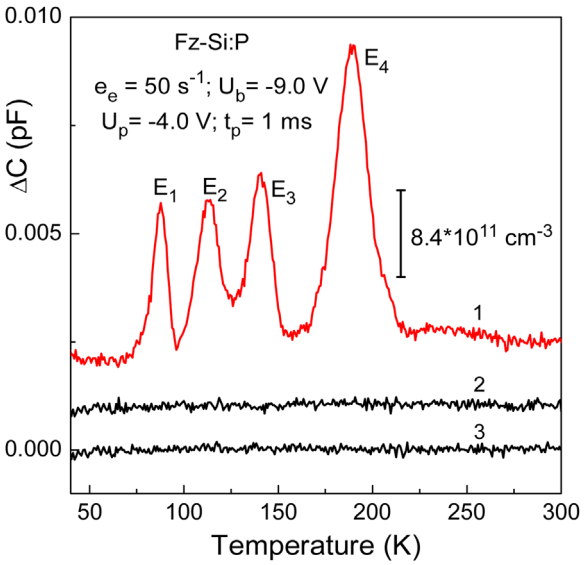

Figure 7 DLTS spectra for samples with an initial resistivity of 1 $\Omega \cdot$cm cut from an n-type FZ silicon wafer (manufacturer B2). Spectra 1 and 2 correspond to samples annealed in oxygen for 30 min at 500 °C, which were cut from the centre and edge parts of the wafer respectively. Spectrum 3 corresponds to a sample cut from the centre of the wafer and then annealed in oxygen for 30 min at 950 °C followed by an anneal at 500 °C. Measurement settings are given on the graph. Spectra 1 and 2 are shifted on the vertical axis for clarity. The corresponding electron activation energies for E_1, E_2, E_3 and E_4 are 0.159 ± 0.002, 0.20 ± 0.002, 0.284 ± 0.002, 0.356 ± 0.002 eV, respectively.

vacancy defect has been permanently annihilated, consistent with the PL images of Fig. 5 and confirmed by DLTS measurements in Section 5.

Finally, returning to Fig. 2 and the lifetime dependence with annealing temperature (200–1100 °C), it is interesting to note that for nitrogen lean silicon wafers, their trend in lifetime is quite different to those samples which contain larger concentrations of nitrogen. Although the lifetime does decrease upon heat-treatments at 450–700 °C, the recovery in lifetime does not occur until a temperature of ≥900 °C is achieved. One reason for this difference could be a higher void concentration (lack of nitrogen to suppress void formation), which can occur when nitrogen lean silicon crystals are pulled quickly [9, 18, 19]. Thus from Fig. 2 it is clear that nitrogen doping does influence the minimum temperature at which the defect can be permanently annihilated. In contrast, however, nitrogen-doped silicon wafers tend to exhibit much higher recombination (compared to N-lean wafers) when heat-treated over the temperature range 450–700 °C, as seen in Fig. 2. Irrespective of the differences between nitrogen-doped and nitrogen-lean FZ silicon, the defect can be permanently removed, and lifetime recovered when FZ silicon wafers are subject to very high temperature (1100 °C) anneals.

5 Observation of electrically active centres with deep levels by DLTS Figure 7 compares conventional DLTS spectra recorded on samples from the central and edge parts of a 1 $\Omega \cdot$cm n-type FZ silicon wafer. Spectra 1 and 2 in Fig. 7 correspond to samples annealed in oxygen for 30 min at 500 °C, which were cut from the centre and edge parts of the wafer respectively. Spectrum 3 of Fig. 7 corresponds to a sample cut from the centre of the wafer and then annealed in oxygen for 30 min at 950 °C followed by an anneal at 500 °C.

An analysis of Spectrum 1 presented in Fig. 7 shows that a 30 min heat-treatment in oxygen at 500 °C resulted in the introduction of the E_1–E_4 traps in the central parts of the wafer, consistent with the PL images of Figs. 4 and 5. A detailed study of majority and minority capture cross sections has not been carried out for the E_1–E_4 traps but from an analysis of their concentrations and positions of energy levels in the gap it can be suggested that at least one of these traps is responsible for the degradation of the minority carrier lifetime upon annealing in the temperature range 450–700 °C (Fig. 1). Furthermore, considering the defect distribution shown in Figs. 4 and 5 indicates that the E_1–E_4 traps measured in the centre of the wafer relate to vacancy defects.

The absence of the traps in Spectrum 2 (the edge region of the wafer) annealed at 500 °C is consistent with a higher lifetime around the periphery, however, as indicated by Fig. 4 and Refs. [6, 8], the periphery lifetime is also reduced compared to those samples annealed at 1000 °C. Therefore, given the discrepancy between lifetime and DLTS measurements on samples from the edge of the wafer, it is not clear at this time what the source of recombination in the lifetime (and PL) measurements is.

The measurement of Spectrum 3 (central region sample) in Fig. 7 provides two significant insights: (i) a high temperature anneal at 950 °C removes the defects giving rise to the E_1–E_4 traps, which is consistent with the lifetime measurements of Figs. 2, 5 and 6 and (ii) the absence of traps

in Spectrum 3 after a subsequent anneal at 500 °C indicates the vacancy defects, which become highly recombination active upon heat-treating at 500 °C, have been permanently annihilated, consistent with the PL image of Fig. 5 and the lifetime measurements of Fig. 6.

6 Conclusions When commercially available FZ silicon wafers were annealed at 450–700 °C in dry oxygen, the lifetime was found to degrade by more than one order of magnitude. PL imaging of nitrogen-doped samples annealed at 500 °C revealed circular patterns of recombination active defects, with higher recombination activity occurring in the centre of the wafer, and far less around the periphery. DLTS measurements on samples extracted from the centre of an n-type FZ silicon wafer annealed at 500 °C revealed a large variety of defects with activation energies ranging from 0.16 to 0.36 eV, however, for samples extracted from the edge of the wafer, no defects could be observed, consistent with our PL images. Our measurements suggest that vacancy related defects are causing the severe degradation in lifetime when FZ wafers are annealed at 450–700 °C.

Upon annealing nitrogen doped FZ silicon at temperatures >800 °C, the lifetime is completely recovered, whereby the defect-rich regions vanish and do not reappear upon subsequent annealing at 500 °C (permanently annihilated), as demonstrated by our PL images, lifetime and DLTS measurements. For nitrogen-lean FZ silicon, much higher temperatures of 1100 °C are required to permanently remove the defect and recover the lifetime, which may correlate with a higher void concentration.

Our results indicate that, in general, FZ silicon should not be assumed to be defect lean, nor can it be assumed that the bulk lifetime will remain stable during thermal processing. Therefore, to retain stable high bulk lifetimes, which is essential for high efficiency solar cells and power devices, thermal processing must be carefully designed.

Acknowledgements This work has been supported by the Australian Renewable Energy Agency (ARENA) fellowships program and the Australian Research Council (ARC) DECRA and Future Fellowships programmes. Responsibility for the views, information or advice expressed herein is not accepted by the Australian Government. The work in UK has been supported by EPSRC (grant EP/M024911/1).

References

[1] J. Haunschild, I. E. Reis, J. Geilker, and S. Rein, Phys. Status Solidi RRL **5**, 199 (2011).
[2] J. D. Murphy, K. Bothe, M Olmo, V. V. Voronkov, and R. J. Falster, J. Appl. Phys. **110**, 053713 (2011).
[3] J. D. Murphy, R. E. McGuire, K. Bothe, V. V. Voronkov, and R. J. Falster, Sol. Energy Mater. Sol. Cells **120**, 402 (2014).
[4] J. D. Murphy, M. Al-Amin, K. Bothe, M. Olmo, V. V. Voronkov, and R. J. Falster, J. Appl. Phys. **118**, 215706 (2015).
[5] N. E. Grant, F. E. Rougieux, D. Macdonald, J. Bullock, and Y. Wan, J. Appl. Phys. **117**, 055711 (2015).
[6] N. E. Grant, F. E. Rougieux, and D. Macdonald, Solid State Phenom. **242**, 120 (2016).
[7] F. E. Rougieux, N. E. Grant, C. Barugkin, D. Macdonald, and J. D. Murphy, IEEE J. Photovolt. **5**, 495 (2015).
[8] N. E. Grant, V. P. Markevich, J. Mullins, A. R. Peaker, F. Rougieux, and D. Macdonald, Phys. Status Solidi RRL **10**, 443–447 (2016).
[9] T. Abe, J. Cryst. Growth **334**, 4 (2011).
[10] N. E. Grant, K. R. McIntosh, and J. T. Tan, J. Solid State Sci. Technol. **1**, P55 (2012).
[11] N. E. Grant, J. Vis. Exp. **107**, e53614 (2016).
[12] R. A. Sinton and A. Cuevas, Appl. Phys. Lett. **69**, 2510 (1996).
[13] L. Dobaczewski, A. R. Peaker, and K. Bonde Nielsen, J. Appl. Phys. **96**, 4689 (2004).
[14] E. Yablonovitch, D. L. Allara, C. C. Chang, T. Gmitter, and T. B. Bright, Phys. Rev. Lett. **57**, 249 (1986).
[15] A. B. Sproul, J. Appl. Phys. **76**, 2851 (1994).
[16] A. L. Blum, J. S. Swirhun, R. A. Sinton, F. Yan, S. Herasimenka, T. Roth, K. Lauer, J. Haunschild, B. Lim, K. Bothe, Z. Hameiri, B. Seipel, R. Xiong, M. Dhamrin, and J. D. Murphy, IEEE J. Photovolt. **4**, 525 (2014).
[17] A. Richter, S. W. Glunz, F. Werner, J. Schmidt, and A. Cuevas, Phys. Rev. B **86**, 165202 (2012).
[18] T. Abe and T. Takahashi, J. Cryst. Growth **334**, 16 (2011).
[19] V. V. Voronkov, J. Cryst. Growth **59**, 625 (1982).